Spin configuration in a frustrated ferromagnetic/antiferromagnetic thin-film system

T K Yamada[1]**, E Martínez**[2]**, A Vega**[3]**, R Robles**[4]**, D Stoeffler**[5]**, A L Vázquez de Parga**[6]**, T Mizoguchi**[1] **and H van Kempen**[7]

[1] Faculty of Science, Gakushuin University, 171-8588 Mejiro, Tokyo, Japan

[2] Fachbereich Physik, Universität Osnabrück, D-49069 Osnabrück, Germany

[3] Departamento de Física Teórica, Atómica y Óptica, Universidad de Valladolid, 47011 Valladolid, Spain

[4] Department of Physics, Uppsala University, SE-75121, Sweden

[5] Institut de Physique et Chimie des Matériaux de Strasbourg (UMR C7504 CNRS-ULP), Strasbourg, France

[6] Departamento de Física de la Materia Condensada, Universidad Autónoma de Madrid, Cantoblanco 28049, Madrid, Spain

[7] Institute for Molecules and Materials, Radboud University, Toernooiveld 1, 6525 ED Nijmegen, The Netherlands

E-mail: edmartin@uos.de

Abstract

We have studied the magnetic configuration in ultrathin antiferromagnetic Mn films grown around monoatomic steps on an Fe(001) surface by spin-polarized scanning tunnelling microscopy/spectroscopy and *ab initio*-parameterized self-consistent real-space tight-binding calculations in which the spin quantization axis is independent for each site, thus allowing noncollinear magnetism. Mn grown on Fe(001) presents a layered antiferromagnetic structure. In the regions where the Mn films overgrows Fe steps the magnetization of the surface layer is reversed across the steps. Around these defects a frustration of the antiferromagnetic order occurs. Due to the weakened magnetic coupling at the central Mn layers, the amount of frustration is smaller than in Cr, and the width of the wall induced by the step does not change with the thickness, at least for coverages up to seven monolayers.

(Some figures in this article are in colour only in the electronic version)

1. Introduction

The interface of ferromagnetic and antiferromagnetic material is important from a scientific point of view because the competing ferromagnetic and antiferromagnetic interactions may lead to complex configurations, particularly when there is frustration in the system. In particular, when an antiferromagnetic layer is deposited on a ferromagnetic substrate with an atomic step ('hidden atomic step') the magnetic frustration around this extended defect can give rise to interesting magnetic structures [1–4]. Due to the localized

nature of the frustrations, it has not been possible to resolve the spin configurations until the introduction of the spin-polarized scanning tunnelling microscopy/spectroscopy (SP-STM/STS) [5].

This problem is also important from the technological point of view. Exchange bias is one of the phenomena associated with the exchange anisotropy created at the interface between an antiferromagnetic material and a ferromagnetic material. Materials exhibiting exchange bias have been used in several practical applications since their discovery [6–8]. In the world of magnetic devices, the goal is to get smaller.

 1

The smaller the space that one bit of information occupies, the more data you can get into a device. Between two magnetic domains with opposite magnetization directions there always exists a domain wall. Therefore a deep understanding of the parameters that control the domain wall width are crucial in order to achieve higher density for data storage.

Mn is exactly in the middle of the 3d transition metal series, just between Fe, which is a natural ferromagnet in the bulk, and Cr, which is an antiferromagnet. Therefore, Mn stands as one of the more complex 3d transition metals from the point of view of the magnetic coupling, and it is a clear candidate to exhibit a great variety of magnetic structures. Mn systems have been experimentally investigated by spin-polarized electron energy-loss spectroscopy [9], scanning electron microscopy with polarization analysis [10] and SP-STM/STS [11, 12]. A layered antiferromagnetic (LAF) arrangement was found in Mn film. Recently, some of the authors [13] have studied the same system using the *ab initio* tight-binding linear muffin-tin orbital (TB-LMTO) method [14], assuming the experimental interlayer distances and a p(1 × 1) magnetic arrangement at the surface, as experimentally observed [11]. Different magnetic solutions with energy differences of a few meV were obtained, with the LAF configuration the less energetic state, in good agreement with the experiments. The LAF as well as the closest metastable solutions had some common features: (i) parallel coupling at the interface between Mn and Fe, (ii) antiparallel coupling between the Mn-surface and subsurface layers and (iii) antiparallel coupling between the two Mn layers closest to the interface. This set of solutions only differs in the couplings at the central Mn layers, that are parallel or antiparallel depending on the Mn thickness, which makes these systems clear candidates to exhibit noncollinear magnetic arrangements under structural defects like monoatomic steps. Using theory, Hafner and Spišák [15] have found complex magnetic coupling in Mn films on Fe(001) allowing atomic relaxations, obtaining an in-plane antiferromagnetic structure.

In this paper, the magnetic structure of thin Mn films grown on Fe(001) is studied. In particular, we focus our attention on the magnetic structure of the Mn films around steps on the Fe(001) substrate. In section 2, by means of SP-STM/STS, we measure in real space and with high spatial resolution the magnetic structure of the films around these defects. The experimental results are interpreted, in section 3, with the help of *ab initio*-parameterized self-consistent real-space tight-binding (TB) calculations in which the spin quantization axis is independent for each site, thus allowing noncollinear magnetism. Throughout the paper, comparisons are made with the Cr/Fe(001) system to get a deeper understanding of which material parameters are crucial for determining the resulting magnetic structure. Finally, in section 4 we summarize our conclusions.

2. Experimental results

All measurements were performed in an ultra-high vacuum (UHV) chamber ($\sim 5 \times 10^{-11}$ mbar) at room temperature (RT). An STM was attached to the chamber, which is equipped with molecular beam epitaxy, Auger spectroscopy, field-emission spectroscopy, sample heating and sputtering facilities [11].
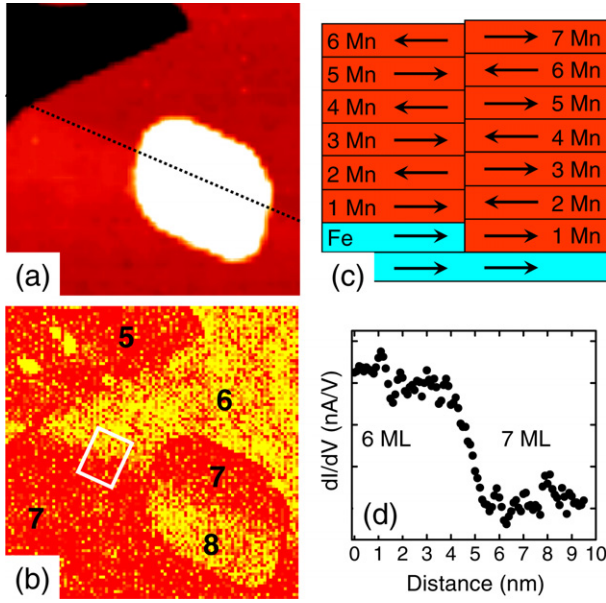
W tips were cleaned by Ar sputtering and annealing and then covered with 10 nm Fe. SP-STS measurements were performed in two different ways: in the first one, $I(V)$ curves were obtained at every pixel of a constant-current topographic image and then numerically differentiated. In the second one, dI/dV maps were obtained with a lock-in amplifier modulating the sample bias voltage by 40 mV at 2 kHz.

The growth conditions are very important because Mn and Fe tend to intermix and the magnetic properties of the Mn are very sensitive to the atomic structure [16]. In this work, Mn was grown on an Fe(001) whisker at $100\,^\circ$C at a rate of 0.6 nm min^{-1}, and the surface topography and electronic structure was characterized by means of scanning tunnelling microscopy/spectroscopy (STM/STS) at RT in UHV using a clean W tip. Atomically and chemically resolved STM images show that the Mn film grows with the same in-plane lattice constant as Fe(001) and that the Fe atoms intermix with the first, the second, and the third Mn layer. The concentration of intermixed Fe decreased with film thickness. Furthermore, STM shows that the growth mode changes from layer-by-layer to layer-plus-islands for coverages higher than 4 ML (monolayers) of Mn. If the temperature of the substrate is increased by a few degrees, this transition from layer-by-layer to layer-plus-islands growth takes place for thicker Mn layers, and the intermixed Fe is present in more Mn layers. Based on apparent step height measurements, made by choosing the bias voltage carefully to avoid the influence of the electronic structure on the results, we conclude that the first two Mn overlayers show significant higher step heights than the Fe single step and that the Mn film relaxes by about 0.02 nm at the third layer. From the fourth layer the interlayer spacings are geometrically the same (about 0.165 nm) and the structure is a body-centred tetragonal (bct) structure [17]. This bct Mn(001) has a layered antiferromagnetic arrangement [10, 11].

When a Mn film is grown across an Fe step (hidden), the Mn film tends to produce a flat surface. We always find steps 0.02 nm high, which corresponds to the difference between the interlayer distances for Fe and Mn. Across one of these steps, the Mn thickness changes by one layer (see figure 1(c)). Due to the LAF structure, the magnetization of the surface layer is reversed across these steps. dI/dV maps obtained with clean W tips around these defects show the same electronic structure on both sides. However, when using Fe-covered W tips, a contrast of magnetic origin is obtained across the hidden step, as can be seen in figure 1(b). The average profile measured in the white box shown in panel (b) can be seen in panel (d), and it gives a domain wall width of around 1.16 nm (2–4 lattice parameters).

To study the possible influence of the set-point values on the observed domain width, we systematically changed the set-point voltage and set-point current. Firstly, the set-point currents were varied with fixed set-point voltage, and thus with varying tip–sample distance (figure 2(a)). In addition, the set-point voltage and current were varied such that the tunnelling resistance stayed constant, and thus with approximately constant tip–sample separation (figure 2(b)). From the results given in figures 2(a) and (b), we can conclude that our values for the domain wall width do not depend on the particular set point used.

In figure 2(c) we show the result of 40 measurements taken with six different magnetic tips for hidden steps covered

Figure 1. (a) STM image after deposition of 5 Mn ML (70×70 nm^2). The dotted line marks the position of the hidden step. (b) dI/dV map taken at $+0.2$ V. The numbers indicate the Mn local thickness. (c) Model of the Mn structure around the hidden step. (d) Average experimental profile across the hidden step measured inside the white box shown in (b).

by different Mn thicknesses. There is no clear dependence between the width of the domain wall and the thickness of the Mn film in the range explored. The error bars in these measurements simply reflect the fact that the tips are different and the resolution of the magnetic images is affected.

3. Theoretical results

For the theoretical investigation of our samples, it is important to point out that when defects are present, as in this system, with the consequent lack of symmetry and hundreds of inequivalent sites, real-space methods with reasonable
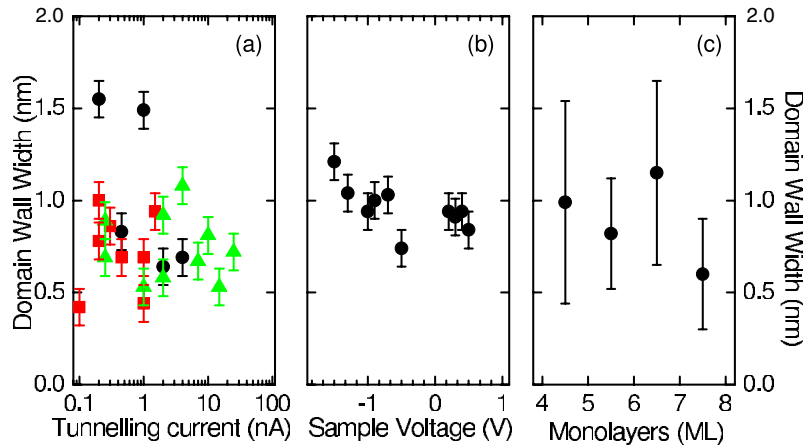
computer requirements are demanded. We have employed an *ab initio*-parameterized self-consistent real-space tight-binding method in which the spin quantization axis is independent for each site, thus allowing noncollinear magnetism. This method has been recently developed and used satisfactorily for the study of supported Cr films on Fe substrates with monoatomic steps [18]. The Hamiltonian in our method can be split into a band term H_{band} and an exchange term H_{exch}, which in the orthogonal $|i\alpha\rangle$ basis of atomic site i and orbital α and with the usual notation are
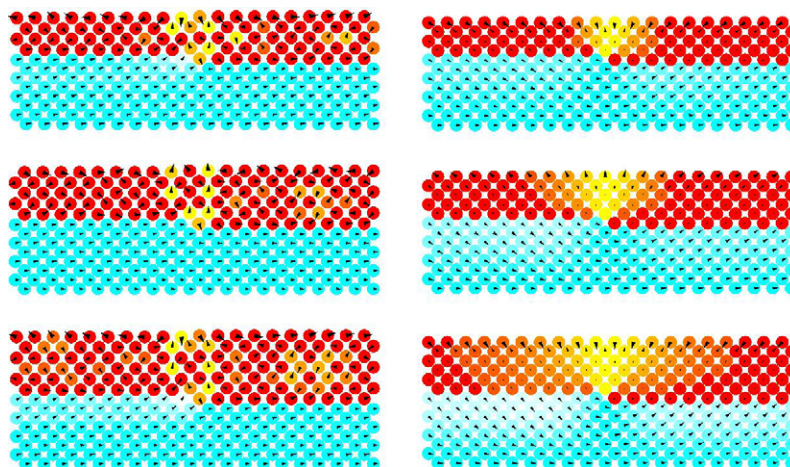
$$H = H_{\text{band}} + H_{\text{exch}} \tag{1}$$

$$H_{\text{band}} = \sum_{\substack{i,j \\ \alpha,\beta}} [(\epsilon_{i\alpha}^0 + U_{i\alpha,j\beta}\langle \hat{n}_{jb} \rangle + Z_i \Omega_{i\alpha})\delta_{ij}\delta_{\alpha\beta}$$

$$+ t_{ij}^{\alpha\beta}(1 - \delta_{ij})]|i\alpha\rangle\langle j\beta| \begin{bmatrix} 1 & 0 \\ 0 & 1 \end{bmatrix}$$

$$H_{\text{exch}} = \sum_{i,\alpha} (-\tfrac{1}{2}J_{i\alpha}\mu_{i_\alpha})|i\alpha\rangle\langle i\alpha| \begin{bmatrix} \cos\theta_i & e^{-i\phi_i}\sin\theta_i \\ e^{i\phi_i}\sin\theta_i & -\cos\theta_i \end{bmatrix}$$

H_{band} contains both the non-diagonal matrix elements (hopping integrals, $t_{ij}^{\alpha\beta}$, between orbitals α and β of different sites i and j, which are assumed to be spin independent) and the spin-independent part of the diagonal matrix elements ($\epsilon_{i\alpha}^0 + U_{i\alpha,j\beta}\langle \hat{n}_{jb} \rangle + Z_i \Omega_{i\alpha}$), being the sum of the local level $\epsilon_{i\alpha}^0$, the electrostatic level shift $U_{i\alpha,j\beta}\langle \hat{n}_{jb} \rangle$ accounting for the charge variations parameterized by the Coulomb integral $U_{i\alpha,j\beta}$ and the crystal-field potential $Z_i \Omega_{i\alpha}$, where Z_i is the local atomic coordination of site i. H_{exch} describes the magnetic part, through the exchange parameter $J_{i\alpha}$ multiplied by the magnitude of the local magnetic moment, $\mu_{i\alpha}$, whose direction is given by the angles (θ_i, ϕ_i) in the spin-rotation matrix. The spin–orbit contribution is not considered here. The Hamiltonian has been parameterized to DFT TB-LMTO calculations of thin Mn films supported on ideal Fe(001) [13] in order to take into account the effects of surface, interface and bulk. The transferability of the parameterization has been checked in systems of 6 and 7 Mn ML on Fe(001), comparing the results with those obtained with the TB-LMTO method [13], finding similar values for the energy differences and magnetic moments.

Figure 2. (a) shows the domain wall width versus the tunnelling current (tip–sample separation). (Black) dots, (green) triangles and (red) squares were obtained at a voltage set point of $V_s = +1.5$ V, $V_s = +0.8$ V, and $V_s = -1.0$ V, respectively. (b) shows the domain wall width versus bias voltage. The experiments were done on hidden steps between 4–5 and 6–7 ML. (c) Domain wall width versus Mn thickness.
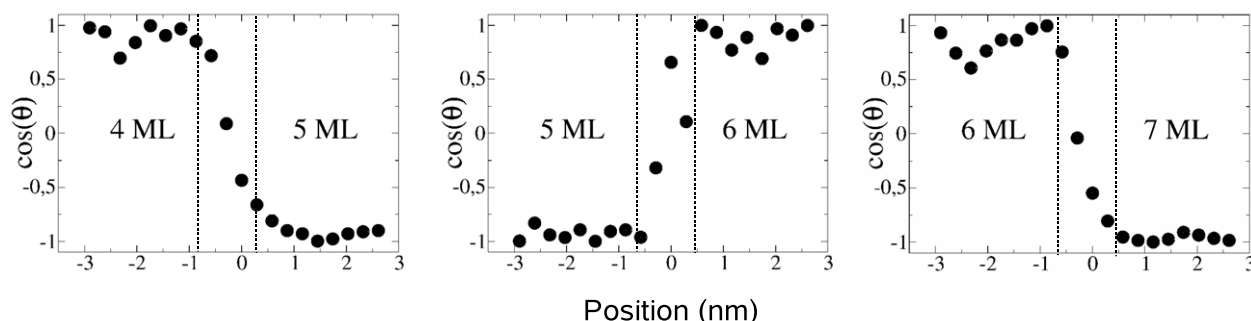
Figure 3. Result of the calculation performed for 4–5, 5–6 and 6–7 monolayers of Mn (left panel) and Cr (right panel) supported on an Fe(001) substrate with a monoatomic step (only a portion of the calculated systems is represented). The arrows indicates the orientation of the individual magnetic moment and its size is proportional to absolute value of the local magnetic moment (average values of the magnetic moments far from the step: $\mu_{Fe}^{bulk} = 2.32\ \mu_B$, $\mu_{Mn}^{surf} = 3.84\ \mu_B$, $\mu_{Cr}^{surf} = 3.07\ \mu_B$, $\mu_{Mn}^{inter} = 2.85\ \mu_B$, $\mu_{Cr}^{inter} = 1.13\ \mu_B$). The colour of the circles is given by the absolute value of the cosine of the angle of the magnetic moment. For Mn and Cr red means a LAF arrangement and yellow indicates the magnetic moment at 90°. For the Fe(001) substrate the blue colour indicates a ferromagnetic arrangement and light blue a deviation from that.
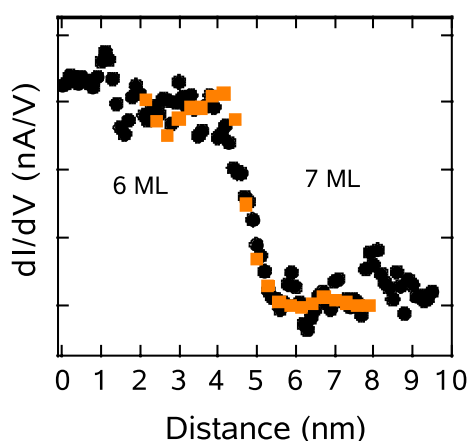
We have simulated the systems represented in figure 1. Despite the preservation of the symmetry in the axis parallel to the step, which can be justified by the length of the observed steps in the system, we have about 40 000 atoms and up to 600 inequivalent sites to describe the semi-infinite system. We have considered coverages of 4–5, 5–6 and 6–7 Mn ML. In all cases, a small step of about 0.02 nm at the surface is present (as experimentally observed). In figure 3 (left panel) we illustrate the noncollinear magnetic moment distributions obtained in the calculations (only a portion of the semi-infinite system is shown). To understand the origin of the noncollinear magnetic arrangement, we have also performed TB collinear restricted calculations (not shown), obtaining different magnetic arrangements, the least energetic one displaying the LAF order at both sides far from the step, while just over the step, due to the impossibility of reaching LAF order together with the parallel coupling at the interface in the whole system, magnetically frustrated atoms were present. Previous studies of Cr/Fe interfaces with steps [18] have shown that this type of frustration in a collinear framework leads the system to drastically reduce the magnetic moments in the frustrated region. However, this moment reduction in the case of Mn is much less noticeable, which is consistent with the fact that the magnetic couplings between Mn layers are weaker and less defined than in Cr, for which the LAF solution is the only one present [18]. The noncollinear magnetic solutions shown in figure 3 are energetically more stable than the collinear ones in all cases, and they reproduce the experimentally observed magnetic contrast at the surface between both sides of the step. This is due to the propagation of the magnetic frustration originated at the interface step. Far from the step, the system tends to preserve the magnetic couplings found in the ideal Mn films on Fe(001) [13], that is the LAF with parallel Fe–Mn coupling at the interface and antiparallel coupling between Mn surface and subsurface layers. Moreover, the tendency of Mn to couple both parallel and antiparallel in the central

layers of the ideal Mn films on Fe(001) is also reflected in the noncollinear arrangements shown in figure 3.

Let us now come to the analysis of the domain-wall evolution as a function of the Mn coverage, in particular the width of the domain wall. Experimentally, we have found a domain-wall width of about 2–4 lattice parameters independently of the Mn coverage. Our theoretical results (figure 3) are also consistent with the experimental finding, as can be deduced from figures 4 and 5, where the cosine of the angle of the local surface magnetic moment with respect to the bulk is plotted through the step (red squares). The central Mn layers decouple the surface from the interface to a large extent, and make these systems behave in a radically different way from what would be expected if one assumes for Mn the magnetic coupling of a typical antiferromagnet like Cr and the associated magnetic frustrations when interfaced with stepped Fe. In fact, we have already indicated before that Mn and Cr have different magnetic behaviour when deposited on an atomically flat Fe(001) surface. The magnetic decoupling of the surface layers from the deeper layers coupled to the substrate has been also proposed recently by Hafner and Spišák [15]. This provides further support to our results. For large enough coverages it is expected that Mn will undergo a structural transition [19] with no magnetic domains at the surface. Our results contrast, however, with those obtained by Schlickum *et al* [12]. These authors found an increase of the domain-wall width on increasing Mn coverage. Growth conditions are very important for the final structure. In these experiments we grew the Mn films about ten times faster than Schlickum *et al* [12]. The faster deposition rate for the same sample temperature may lead to a smaller level of intermixing between Mn and Fe and therefore to a different magnetic structure. Furthermore, Schlickum *et al* [12] explained their results using a simple Heisenberg model for localized magnetism [12], assuming that Mn behaves like Cr and considering the same exchange parameter for Mn–Fe and Mn–Mn.

Figure 4. Cosine of the angle of the magnetic surface moments with respect to the bulk obtained in the theoretical calculations shown in figure 3 for 4–5, 5–6 and 6–7 ML. Vertical dashed lines specify the size of the domain wall in each case.

Figure 5. (black dots) Average experimental profile across the hidden step measured inside the white box shown in figure 1(b). (orange squares) Cosine of the angle of the magnetic surface moments with respect to the bulk obtained in the theoretical calculation shown in figure 3 for 6–7 ML.

In order to further illustrate the different magnetic behaviour of Mn and Cr, we have performed the same type of calculation in similar systems, but with Cr instead of Mn deposited on the stepped Fe substrate and the corresponding interatomic distances (figure 3, right panel). The difference between the noncollinear arrangements in Mn/Fe and Cr/Fe is clear. The strong antiferromagnetic character of Cr leads to strong magnetic frustrations that are propagated towards the surface occupying a region in which the best compromise to the antiparallel Cr–Cr and Cr–Fe couplings is achieved. As a result, the domain-wall width increases with increasing Cr coverage and the frustration is partially released in the Fe(001) substrate.

4. Conclusions

In conclusion, we have investigated the magnetic structure on thin Mn films grown on an Fe(001) surface with a monoatomic step. In our SP-STM images we found a change in the magnetic contrast when crossing one of those steps due to the change of the Mn thickness. We have found that the width of the domain wall around the substrate steps does not depend on the thickness, at least for coverages up to seven

Mn overlayers, and it is about two lattice parameters. This is due to the weakly defined magnetic coupling at the central Mn layers that decouple the surface from the interface to a large extent. We compare our findings for the Mn films with the behaviour of Cr films. In contrast to Mn, ideal Cr films have strong antiferromagnetic couplings and longer range order than in Mn, up to the point that only one magnetic arrangement in the system has been found in the collinear framework, corresponding to an LAF configuration. This strong coupling produces a high amount of frustration on steps and as a consequence in the case of Cr the domain-wall width increases with the coverage.

Acknowledgments

References

[1] Berger A and Hopster H 1994 *Phys. Rev. Lett.* **73** 193
[2] Vega A, Demangeat C, Dreyssé H and Chouairi A 1995 *Phys. Rev. B* **51** 11546
[3] Stoeffler D and Gautier F 1995 *J. Magn. Magn. Mater.* **147** 260
[4] Berger A and Fullerton E E 1997 *J. Magn. Magn. Mater.* **165** 471
[5] Bode M, Getzlaff M and Wiesendanger R 1998 *Phys. Rev. Lett.* **81** 4256
[6] Prinz G A 1998 *Science* **282** 1660
[7] Nogués J and Schuller I K 1999 *J. Magn. Magn. Mater.* **192** 203
[8] Wolf S A, Awschalom D D, Buhrman R A, Daughton J M, von Molnar S, Roukes M L, Chtchelkanova A Y and Treger D M 2001 *Science* **294** 1488
[9] Walker T G and Hopster H 1993 *Phys. Rev. B* **48** 3563
[10] Tulchinsky D A, Unguris J and Celotta R J 2000 *J. Magn. Magn. Mater.* **212** 91
[11] Yamada T K, Bischoff M M J, Heijnen G M M, Mizoguchi T and van Kempen H 2003 *Phys. Rev. Lett.* **90** 056803
[12] Schlickum U, Janke-Gilman N, Wulfhekel W and Kirschner J 2004 *Phys. Rev. Lett.* **92** 107203
Wulfhekel W, Schlickum U and Kirschner J 2005 *Micros. Res. Tech.* **66** 105

[13] Martínez E, Vega A, Robles R and Vázquez de Parga A L 2005 *Phys. Lett.* A **337** 469
[14] Andersen O K and Jepsen O 1984 *Phys. Rev. Lett.* **53** 2571
[15] Hafner J and Spišák D 2005 *Phys. Rev.* B **72** 144420
[16] Wu R and Freeman A J 1996 *J. Magn. Magn. Mater.* **161** 89
[17] Yamada T K, Bischoff M M J, Mizoguchi T and van Kempen H 2002 *Surf. Sci.* **516** 179
[18] Robles R, Martínez E, Stoeffler D and Vega A 2003 *Phys. Rev.* B **68** 094413
[19] Passamani E C, Croonenborghs B, Degroote B and Vantomme A 2003 *Phys. Rev.* B **67** 174424